TRPV4 enhances the cellular uptake of aminoglycoside antibiotics

Takatoshi Karasawa[1], Qi Wang[1], Yi Fu[2,3], David M. Cohen[2,3] and Peter S. Steyger[1,*]

[1]Oregon Hearing Research Center, and [2]Division of Nephrology and Hypertension, Oregon Health and Science University, 3181 Sam Jackson Park Road, Portland, OR 97239, USA
[3]Portland Veterans Affairs Medical Center, 3710 SW US Veterans Hospital Road, Portland, OR 97239, USA
*Author for correspondence (e-mail: steygerp@ohsu.edu)

Accepted 28 May 2008
Journal of Cell Science 121, 2871-2879 Published by The Company of Biologists 2008
doi:10.1242/jcs.023705

Summary

The cochlea and kidney are susceptible to aminoglycoside-induced toxicity. The non-selective cation channel TRPV4 is expressed in kidney distal tubule cells, and hair cells and the stria vascularis in the inner ear. To determine whether TRPV4 is involved in aminoglycoside trafficking, we generated a murine proximal-tubule cell line (KPT2) and a distal-tubule cell line (KDT3). TRPV4 expression was confirmed in KDT3 cells but not in KPT2 cells. Removal of extracellular Ca^{2+} significantly enhanced gentamicin–Texas-Red (GTTR) uptake by KDT3, indicative of permeation through non-selective cation channels. To determine whether TRPV4 is permeable to GTTR, stable cell lines were generated that express TRPV4 in KPT2 (KPT2-TRPV4). KPT2-TRPV4 cells took up more GTTR than control cell lines (KPT2-pBabe) in the absence of extracellular Ca^{2+}. TRPV4-dependent GTTR uptake was abolished by a point mutation within the crucial pore region of the channel, suggesting that GTTR permeates the TRPV4 channel. In an endolymph-like extracellular environment, clearance of GTTR was attenuated from KPT2-TRPV4 cells in a TRPV4-dependent fashion. We propose that TRPV4 has a role in aminoglycoside uptake and retention in the cochlea.

Supplementary material available online at
http://jcs.biologists.org/cgi/content/full/121/17/2871/DC1

Key Words: Gentamicin, Ototoxicity, Aminoglycosides, Cochlea, Hair cells, Stria vascularis, TRPV4, Drug permeability

Introduction

Aminoglycoside antibiotics are clinically important drugs and frequently used worldwide (Forge and Schacht, 2000). Aminoglycosides are highly effective in treating life-threatening Gram-negative bacterial infections, such as meningitis and bacterial sepsis in infants (Klein, 1984; Grohskopf et al., 2005). Drug entry into bacteria is energy dependent. Active export of cations out of the cytosol hyperpolarizes bacteria, and induces an electrophoretic driving force that promotes the entry of cationic aminoglycosides. A pH gradient between acidic extra-bacterial fluids compared with the more alkaline cytosolic environments of bacteria also contributes to aminoglycoside entry (Taber et al., 1987). In bacteria, aminoglycosides bind to ribosomal RNA and induce mis-translation and inhibition of protein synthesis, resulting in bacterial death (Davies and Davis, 1968; Noller, 1991).

Therapeutic use of aminoglycosides is problematic, because these drugs are also nephrotoxic and ototoxic. Aminoglycoside-induced nephrotoxicity results in increased morbidity during and after treatment, and can cause kidney failure. Acute renal toxicity is largely reversible because kidney tubule cells can proliferate and replace cells lost to aminoglycoside toxicity (Mingeot-Leclercq and Tulkens, 1999). However, ototoxicity is mostly permanent because mammalian inner-ear sensory hair cells do not regenerate following aminoglycoside-induced cytotoxicity (Chen and Segil, 1999; Lowenheim et al., 1999).

Aminoglycoside toxicity occurs through cell death mechanisms that include activation of caspase 3 and caspase 9, formation of reactive oxygen species, and the activation of Jun N-terminal kinases (JNKs) (Lee et al., 2004; Hirose et al., 1997; Pirvola et al., 2000). Since it is difficult to inhibit the variety of cell-death mechanisms that might be induced by aminoglycosides, another strategy to prevent aminoglycoside-induced ototoxicity is to block the entry of the drug into cells. To identify pharmacological blockers of aminoglycoside entry, it is important to understand how cells take up aminoglycosides.

One mechanism by which inner-ear hair cells take up aminoglycosides is endocytosis at the apical membrane (Hashino and Shero, 1995; Hiel et al., 1992). Internalized aminoglycosides are transported into lysosomes, where the drugs accumulate over time and disrupt lysosomes (Hashino et al., 1997). In kidney cells, aminoglycosides are also transported through the Golgi complex and the endoplasmic reticulum (ER) in a retrograde manner, and subsequently released into the cytosol from the ER (Sandoval and Molitoris, 2004).

There is another mechanism of aminoglycoside entry, which is ion channel permeation into cells. In cochlear sensory hair cells, aminoglycosides permeate through the mechanosensitive transduction channels located at the tips of individual stereocilia comprising the hair bundle (Marcotti et al., 2005). In cultured kidney cells, chemical agonists of the TRPV1 channel, low extracellular Ca^{2+} levels, negative cellular potentials or acidic extracellular pH enhance the rapid cellular uptake of aminoglycosides, suggesting that they permeate through cation channels (Myrdal and Steyger, 2005; Meyers et al., 2003).

Endocytosis is temperature-dependent in euthermic birds and mammals (37-38°C in mammals) and slows down at hypothermic temperatures (Mamdouh et al., 1996). However, rapid aminoglycoside uptake and toxicity occur at room temperature and

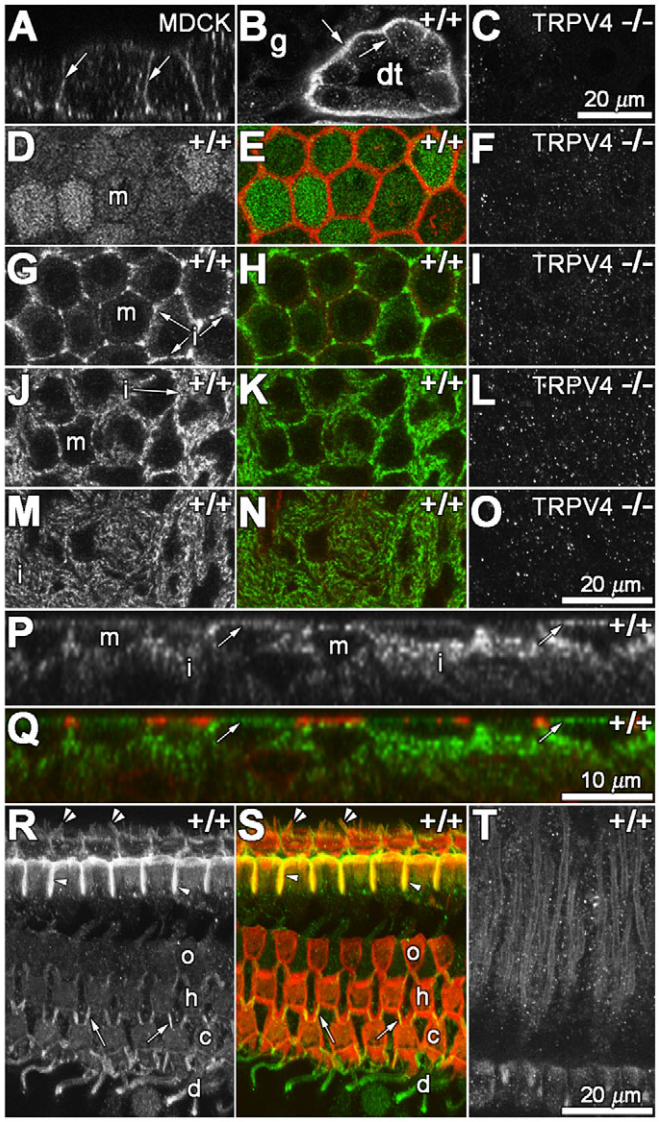

Fig. 1. (A-T) TRPV4 expression in kidney and inner ear. In MDCK cells, TRPV4 immunofluorescence was preferentially localized at the basolateral membrane (arrows in A). TRPV4 was also localized at the basolateral membranes (arrows) of wild-type (+/+) murine kidney distal tubule cells, but not in adjacent glomerular regions (g, in B), nor in the kidney of TRPV4-deficient mice (–/–, in C). In wholemounts of the stria vascularis from wild-type mice, TRPV4 was localized at the lumenal surface of marginal cells (m in D; green in E) at the level of the actiniferous tight junctions (red) between adjacent marginal cells (E, same focal plane as D). There was negligible TRPV4 immunoexpression at the lumenal surface of marginal cells of TRPV4-deficient mice (F). In a focal series of the cells shown in D and E, below the actiniferous tight junctions, only weak TRPV4 immunofluorescence occurred in the somata of marginal cells, but was prominent at the periphery of marginal cells (i in G, green in H). There was no TRPV4 expression detected in the somata of marginal cells from TRPV4-deficient mice (I). At lower focal planes than in G and H, strong, characteristic TRPV4 expression (J,M, green in K,N) was localized in intermediate (i) cells. TRPV4 expression could not be detected in the intra-strial tissues of TRPV4-deficient mice (L,O). In *z*-sections of the stria vascularis, TRPV4 immunolabeling was clearly associated with the lumenal surface (arrows) of the marginal cells (m), between the actiniferous tight junctions, and in the intermediate cells (i) below the weakly-labeled somata of marginal cells of wild-type mice (P,Q). In the organ of Corti, TRPV4 expression was most prominent in the region of tight junctions between adjacent pillar cells (arrowheads), and also between adjacent Deiters' cell phalangeal apices (arrows; R,S). The stereocilia of inner hair cells displayed TRPV4 expression (double arrowheads; R,S). TRPV4 expression was also present in Deiters' cell phalanges (d), but only weakly in OHCs (ohc) and spiral ganglion cells (T). Scale bar in C also applies for A and B. Scale bar in O also applies for D-N, R-T. Scale bar in Q also applies for P.

also at 4°C in vitro (Myrdal et al., 2005; Myrdal and Steyger, 2005; Hirose et al., 1997), further supporting the hypothesis that aminoglycoside permeates through non-selective cation channels. This probably involves transient receptor potential (TRP) cation channels of the subfamily V, such as TRPV1, because regulators of these channels modulate aminoglycoside uptake (Myrdal and Steyger, 2005).

In the kidney, proximal tubule cells are more sensitive to aminoglycoside-induced cytotoxicity, presumably because these cells take up and retain the drugs. However, distal tubule cells are more resistant to aminoglycosides, most probably because these cells do not retain aminoglycosides in the cytoplasm. One major difference between proximal and distal tubule cells is the expression of TRPV4 (another TRPV channel), which is abundantly expressed in distal tubule cells but not in proximal tubule cells (Strotmann et al., 2000; Tian et al., 2004). TRPV4 is a mechanosensitive receptor that is responsive to systemic osmotic pressure induced by cell swelling in hypo-osmotic medium (Liedtke et al., 2000; Strotmann et al., 2000). In the kidney, TRPV4 is only expressed in water-impermeant nephron segments and in areas where generation of a substantial osmotic gradient can be expected (Tian et al., 2004). In the cochlea, TRPV4 is expressed in hair cells and the stria vascularis (Liedtke et al., 2000; Takumida et al., 2005; Shen et al., 2006). In this study, we characterize TRPV4 expression in the inner ear and kidney, and determine that TRPV4 can mediate aminoglycoside uptake and retention using kidney cell lines. Our data lead us to propose that TRPV4 channels are involved in aminoglycoside uptake and retention in the inner ear.

Results

TRPV4 expression in kidney and inner ear

To determine whether TRPV4 is appropriately located to contribute to aminoglycoside trafficking in the kidney and inner ear, the protein expression of TRPV4 was characterized by immunofluorescence in these tissues. In Madin-Darby canine kidney (MDCK) cells, TRPV4 protein was preferentially localized at the basolateral membrane (Fig. 1A), consistent with the known expression pattern of TRPV4 in kidney (Tian et al., 2004). TRPV4 was also detected in the basolateral membranes of murine kidney distal tubule cells (Fig. 1B), but not in adjacent tubular segments or in the kidney of TRPV4-deficient mice (Fig. 1C). In the inner ear, TRPV4 immunoexpression has been observed in the stria vascularis and organ of Corti (Liedtke et al., 2000; Takumida et al., 2005). In the stria vascularis, TRPV4 was localized at the lumenal surface of marginal cells (Fig. 1D,E,P,Q), and only weakly within their somata (Fig. 1G,H,P,Q). TRPV4 was preferentially localized in intermediate cells (Fig. 1G,H,J,K,M,N,P,Q), which surround the entire basolateral membrane of marginal cells, interdigitating between marginal cells separating them from another, as previously described (Takeuchi et al., 2001). TRPV4 was not detected in the stria vascularis of TRPV4-deficient mice (Fig. 1F,I,L,O).

In the organ of Corti of wild-type mice, TRPV4 expression was most prominent near tight junctions between adjacent pillar cells, and also between adjacent Deiters' cell phalanges (Fig. 1R,S). The stereocilia of inner hair cells displayed a distinct TRPV4 expression

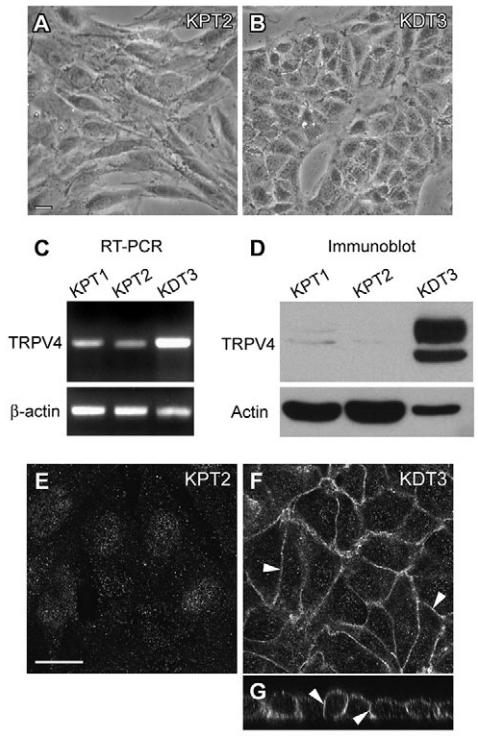

Fig. 2. New kidney cell line generation and TRPV4 expression. By spontaneous immortalization, three cell lines were generated from primary murine kidney cultures. (A,B) Bright-field images show KPT2 cells with a fibroblastic morphology (A), and KDT3 cells with an epithelial (cobblestone-like) appearance and smooth edges to cell clusters (B). (C,D) TRPV4 expression levels were determined by RT-PCR (C) and immunoblotting (D). KDT3 cells showed high levels of TRPV4 whereas KPT1 and KPT2 showed weak TRPV4 expression or possibly non-specific bands. Lower levels of β-actin following RT-PCR (C) and of actin following immunoblotting (D) suggest that KDT3 cells express β-actin and possibly other actin isoforms at lower levels compared with KPT1 and KPT2. (E) Expression of TRPV4 was negligible in KPT2 cells. (F) Immunofluorescence showed TRPV4 localization at the basolateral membrane (arrowheads) of KDT3 cells. (G) Orthogonal view of KDT3 cells shows TRPV4 expression in the basolateral membrane (arrowheads). Scale bars, 20 μm.

pattern (Fig. 1R,S) – in contrast to the outer hair cell (OHC) stereocilia, which showed much weaker TRPV4 expression (data not shown). TRPV4 expression was also localized in Deiters' cell phalanges, and weakly in OHC bodies and spiral ganglion cells (Fig. 1R,T). TRPV4 expression was not detected in the organ of Corti of TRPV4-deficient mice (data not shown).

Generation of a murine kidney cell line and analysis of TRPV4 expression

To compare aminoglycoside uptake between kidney proximal and distal tubule cells, we obtained spontaneously immortalized proximal and distal tubule cell lines from murine kidney. Primary kidney cell cultures were maintained for 3-4 weeks. Out of thirty growing cell colonies that were subcultured, three clones became immortalized. Two cell lines looked alike, showing a fibroblast-like morphology, and a third appeared more epitheloid, with a classic epithelial/cobblestone appearance and smooth edges to cell clusters (Fig. 2A,B). This morphological difference was also reflected in TRPV4 expression levels revealed by reverse transcriptase (RT)-PCR and immunoblotting (Fig. 2C,D). Although RT-PCR detected the TRPV4 transcript in all three cell lines at the expected size (410 bp), the third, epitheloid cell line showed substantially higher levels of *TRPV4* mRNA than the other two (Fig. 2C). The control β-actin band (373 bp), however, showed a lower level of expression in the third cell line compared with the other two (Fig. 2C). In immunoblots, two TRPV4 bands of ~110 kDa were detected in the epitheloid cell line, with the upper one being possible two bands (Fig. 2D). This is consistent with previous reports that the upper band is the glycosylated and/or phosphorylated form(s) (Xu et al., 2003). Similar to the RT-PCR data, the epitheloid cell line showed actin (42 kDa) at a level that is lower than that in the other two cell lines (Fig. 2D). Although the actin antibody detects all the major actin isoforms, including α-, β- and γ-actin, the differences in β-actin levels are probably reflected in the immunoblot. The higher actin expression levels in the first two cell lines possibly originated from high actin expression in the brush border of the kidney proximal tubule. By using confocal microscopy, TRPV4 was seen to be prominently localized at the basolateral membrane of the third cell line – with low expression in the apical membrane (Fig. 2F,G) – but not in the other two cell lines (Fig. 2E). On the basis of both morphology and TRPV4 expression, two cell lines appeared to be proximal-tubule cells, whereas the third TRPV4-expressing cell line was derived from the distal tubule (or collecting duct). We hereafter refer to these cell lines KPT1, KPT2 and KDT3, respectively.

Gentamicin–Texas-Red uptake in kidney cells is enhanced in the absence of extracellular Ca^{2+}

A fluorescent conjugate of gentamicin and Texas Red (GTTR) is useful to study the non-endocytotic aminoglycoside uptake in cells, and its intracellular localization (Myrdal et al., 2005; Myrdal and Steyger, 2005). KPT2 and KDT3 cells were treated with 5 μg/ml GTTR for 30 seconds at room temperature to determine their comparative rate of GTTR uptake. In the presence of physiological levels of extracellular Ca^{2+} (1.25 mM), levels of GTTR fluorescence were low in KPT2 and KDT3 cells, although significantly more GTTR fluorescence was observed in KPT2 cells compared with KDT3 cells (Fig. 3A,B). The intensity of cytoplasmic GTTR fluorescence in KDT3 cells was only 62% of that in KPT2 cells in the presence of extracellular Ca^{2+} (Fig. 3E). Incubation of cells with GTTR in the absence of extracellular Ca^{2+} substantially increased GTTR fluorescence in both cell types (Fig. 3C-E, $P<0.001$, between 1.25 mM and 0 mM Ca^{2+} for both KPT2 and KDT3, respectively). This increase was significantly greater (2.2-fold) in KDT3 cells compared with the 1.5-fold increase in KPT2 cells, resulting in similar uptake levels (Fig. 3C-E). In both KPT2 and KDT3 cells, GTTR fluorescence was diffusely distributed in the cytoplasm and was visible as a punctated pattern within the nucleus, reminiscent of the GTTR-labeled nucleoli described in opossum kidney (OK) and MDCK cells (Myrdal et al., 2005).

These results suggest that aminoglycoside uptake in KDT3 cells is very sensitive to extracellular Ca^{2+} levels, whereas uptake in KPT2 cells is also affected by extracellular Ca^{2+}. Removal of extracellular Ca^{2+} increases inward currents of TRPV4 channels (Voets et al., 2002). It is possible that TRPV4 is a main determinant in aminoglycoside uptake in KDT3 cells, and the GTTR uptake difference in the presence of extracellular Ca^{2+} is due to a reduced inward current through TRPV4 in KDT3 cells. The enhancement of GTTR uptake in KPT2 cells by extracellular Ca^{2+} removal suggests that these cells express other Ca^{2+}-sensitive cation channels that are also permeable for GTTR.

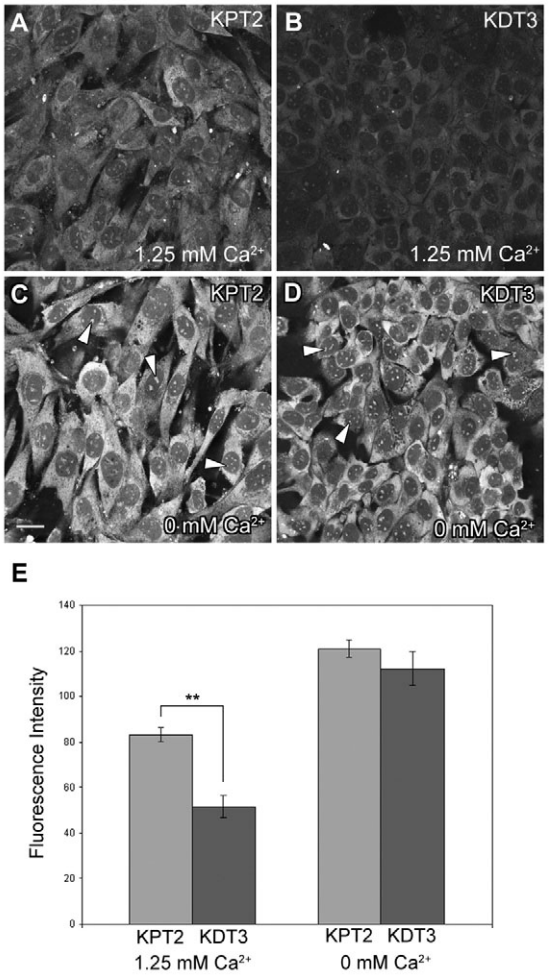

Fig. 3. GTTR uptake is enhanced in the absence of extracellular Ca^{2+}. (A,B) In the presence of extracellular 1.25 mM Ca^{2+}, KPT2 and KDT3 cells had modest and low levels of intracellular GTTR fluorescence, respectively, after 30 seconds of GTTR treatment. (C,D) In the absence of extracellular Ca^{2+}, KPT2 cells showed a modest increase in GTTR fluorescence (C), whereas KDT3 cells showed substantially enhanced GTTR uptake (D). In both KPT2 and KDT3 cells, GTTR fluorescence was diffusely distributed in the cytoplasm, with small puncta (arrowheads) within the nucleus. (E) Fluorescence intensity of cytoplasmic GTTR in KDT3 cells was significantly lower than in KPT2 cells in the presence of extracellular Ca^{2+} (**P<0.01). Removal of extracellular Ca^{2+} greatly enhanced GTTR fluorescence in both KPT2 and KDT3 cells compared with 1.25 mM Ca^{2+} condition (P<0.001). The enhanced GTTR levels by extracellular Ca^{2+} removal were similar between KPT2 and KDT3 cells. Fluorescence intensity data are shown as mean ± s.d. Scale bar, 20 μm.

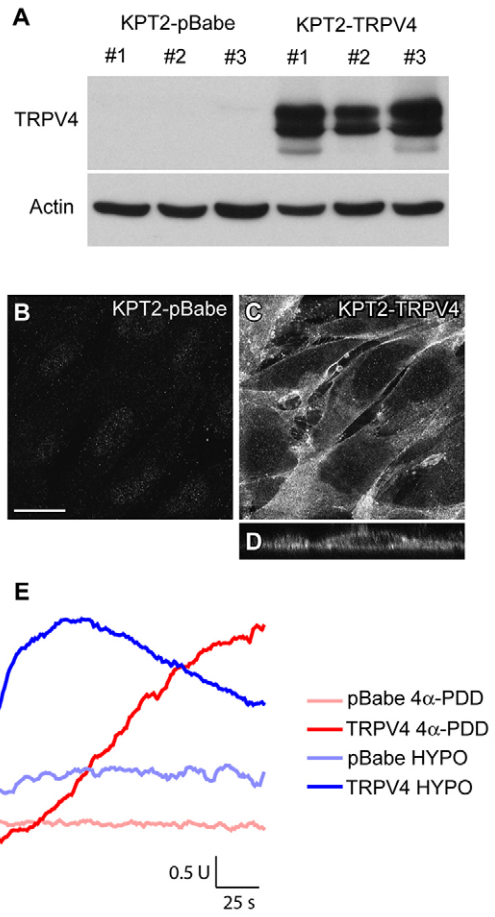

Fig. 4. Generation of KPT2-derived cell lines that express TRPV4. (A) In immunoblots, three empty vector control clones (KPT2-pBabe) did not express TRPV4, whereas three TRPV4-expressing clones (KPT2-TRPV4) highly expressed TRPV4 with two or three bands of ~110 kDa. Actin bands at 42 kDa confirmed that there were similar amounts of total protein in the samples. (B) There was negligible TRPV4 expression in KPT2-pBabe cells. (C) In KPT2-TRPV4 cells, immunofluorescence showed uniform localization of TRPV4 at the cell membrane. (D) Orthogonal view of KPT2-TRPV4 shows that TRPV4 protein expression is uniform in the membrane, including the apical membrane. Scale bar in B also applies for C and D (20 μm). (E) TRPV4-dependent Ca^{2+} entry in response to hypotonic stress or the TRPV4 agonist 4α-PDD was observed in KPT2-TRPV4 cells, but not in KPT2-pBabe cells. Fura-2 fluorescence was monitored as an index of intracellular Ca^{2+} concentration (see Materials and Methods), and the Fura-2 ratio (in arbitrary unit; U) is depicted as a function of time. Arrowhead denotes onset of hypotonic stress or addition of 4α-PDD.

GTTR uptake is enhanced by TRPV4 in the absence of extracellular Ca^{2+}

To test whether the presence of TRPV4 channels enhances GTTR uptake, stable cell lines that express TRPV4 were generated using KPT2 cells. Three KPT2-derived, exogenous TRPV4-expressing cell lines (KPT2-TRPV4) and three vector control cell lines (KPT2-pBabe) were generated, all of which retained parental KPT2 morphology. Immunoblotting and immunofluorescence confirmed expression of TRPV4 in all KPT2-TRPV4 cells, and negligible expression of TRPV4 in KPT2-pBabe cells (Fig. 4A-D). Unlike in KDT3 cells, the upper bands in immunoblots of KPT2-TRPV4 clones were not doublets (Fig. 2D, Fig. 4A). Instead, two clones (#1 and #3) showed a new band of less molecular mass, possibly a truncated form of TRPV4 generated by proteolysis (Fig. 4A). In all three KPT2-TRPV4 cells, TRPV4 expression was uniformly localized at the cell membrane, with some diffuse somatic labeling (Fig. 4C,D). TRPV4 channels can induce Ca^{2+} influx in response to a hypotonic stimulus or to the TRPV4-specific activator 4α-phorbol 12,13-didecanoate (4α-PDD) (Liedtke et al., 2000; Strotmann et al., 2000; Watanabe et al., 2002). To confirm that KPT2-TRPV4 cells express functional TRPV4, Ca^{2+} transients in response to hypotonicity and treatment with 4α-PDD were examined by Fura-2 ratiometry. KPT2-TRPV4 cells exhibited intracellular Ca^{2+} increase in response to hypotonicity or treatment with 4α-PDD with different time courses; peak Ca^{2+} influx occurred at 50 seconds of hypotonicity, whereas Ca^{2+} influx was yet to reach its peak after 160 seconds of 4α-PDD treatment

(Fig. 4E). KPT2-pBabe cells did not respond to either stimulus, confirming that the Ca^{2+} influx observed in KPT2-TRPV4 is dependent on TRPV4 (Fig. 4E).

After a 30-second treatment with GTTR in the presence of extracellular Ca^{2+}, no significant difference in GTTR uptake was seen in all KPT2-TRPV4 and KPT2-pBabe cells (Fig. 5A,B,E). In the absence of extracellular Ca^{2+}, all KPT2-TRPV4 cells took up significantly more GTTR than the three KPT2-pBabe cells (Fig. 5C-E). In the presence of extracellular Ca^{2+}, GTTR uptake levels observed in these KPT2-derived cell lines were slightly higher than those in parental KPT2 cells (data not shown). This might be due to alterations in gene expression caused by puromycin in medium and/or retrovirus used for to generate the cell line. The fluorescence intensity of cytoplasmic GTTR was quantified for KPT2-pBabe and KPT2-TRPV4 cells in the presence and absence of extracellular Ca^{2+} (Fig. 5E). Although there was no significant difference in the mean GTTR levels in the presence of extracellular Ca^{2+}, there was a statistically significant increase (>1.6-fold, $P<0.01$) in KPT2-TRPV4 cells compared with KPT2-pBabe in the absence of extracellular Ca^{2+}.

Mammalian inner-ear endolymph is low in Ca^{2+} (0.023 mM) (Lang et al., 2007), and low extracellular Ca^{2+} levels favor aminoglycoside entry into hair cells in vitro (Marcotti et al., 2005). Low Ca^{2+} (at 0.05 mM) instead of no Ca^{2+} was sufficient to enhance GTTR uptake in KPT2-TRPV4 cells compared with KPT2-pBabe cells (Fig. 5E).

GTTR uptake in KPT2-TRPV4 cells is dependent on TRPV4 channels

KPT2 cell clones that express an M680D point mutant of TRPV4 (KPT2-M680D) were generated to further determine the role of TRPV4 in GTTR uptake. The M680D mutation abolishes Ca^{2+} selectivity in TRPV4 channels by altering the channel-pore properties (Voets et al., 2002; Nilius et al., 2004). Expression of the M680D TRPV4 mutant was localized at the cell membrane and expression levels in KPT2-M680D cells were similar to that of TRPV4 in KPT2-TRPV4 (Fig. 6A-C). After a 30-second GTTR treatment, uptake of GTTR in KPT2-M680D cells was not enhanced following removal of extracellular Ca^{2+}, suggesting that enhanced GTTR uptake in KPT2-TRPV4 cells is probably due to GTTR permeating the pore of the TRPV4 channel (Fig. 6D).

The non-specific TRP-channel inhibitor Ruthenium Red (RR; which blocks cation currents) was administered together with GTTR to further test whether TRPV4 contributes to GTTR uptake in KPT2-TRPV4 cells. After a 30-second GTTR treatment with 50 μM RR in the absence of extracellular Ca^{2+}, GTTR fluorescence levels were significantly lower in KPT2-pBabe and KPT2-TRPV4 cells than those in cells not treated with RR (supplementary material Fig. S1). Although inhibition of GTTR uptake by RR was greater in KPT2-TRPV4 cells, KPT2-pBabe cells also showed significant inhibition of GTTR uptake by RR (supplementary material Fig. S1). It is possible that KPT2-pBabe expresses other non-selective cation channels that are involved in aminoglycoside uptake, and these channels are also inhibited by RR.

GTTR clearance from KPT2-TRPV4 in an endolymph-like extracellular environment

Inner-ear hair cells take up aminoglycosides from endolymph by endocytosis or ion channel permeation (Hashino and Shero, 1995; Marcotti et al., 2005). To determine whether cells can clear aminoglycosides into an endolymph-like extracellular environment,

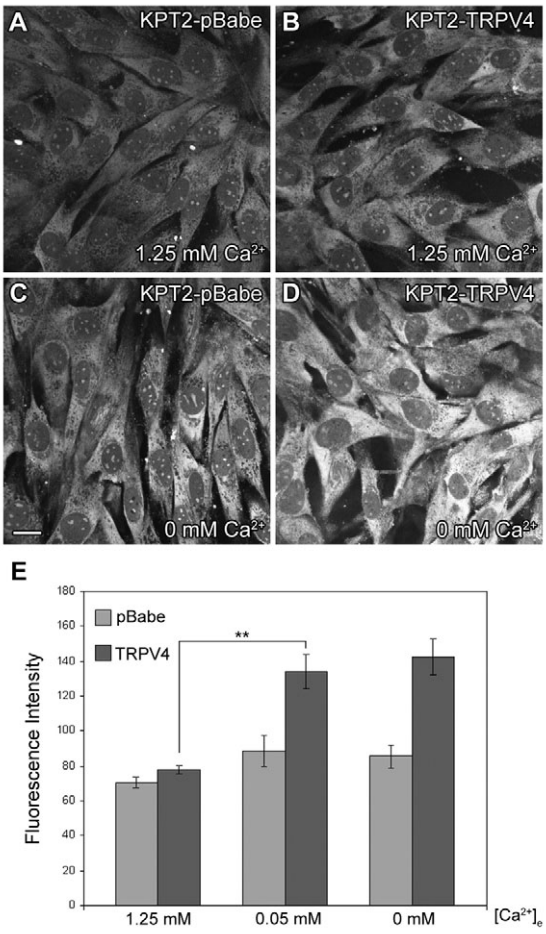

Fig. 5. (A-E) KPT2-TRPV4 cell lines show enhanced GTTR uptake in the absence of extracellular Ca^{2+}. After 30 seconds of GTTR treatment, there was little difference in GTTR uptake between KPT2-TRPV4 and KPT2-pBabe cells in the presence of extracellular Ca^{2+} (A,B), with no significant difference in fluorescence intensity of cytoplasmic GTTR (E). Enhanced GTTR uptake was observed in KPT2-TRPV4 cells in the absence of extracellular Ca^{2+} compared with KPT2-pBabe cells (C,D). Similar results were obtained for all the three KPT2-TRPV4 and three KPT2-pBabe cell lines. Fluorescence intensity of cytoplasmic GTTR in KPT2-TRPV4 cells was significantly higher than in KPT2-pBabe cells under conditions of 0 mM or 0.05 mM extracellular Ca^{2+} (E). Fluorescence intensity data are shown as mean ± s.d. $^{**}P<0.01$. Bar in C also applies for A, B and D (20 μm).

clearance of GTTR from cells was measured by loss of GTTR fluorescence following incubation in endolymph-like buffer (low Na^+, high K^+, low Ca^{2+}). To ensure sufficient GTTR levels in KPT2-pBabe cells at the initial time point, all cells were treated with GTTR in PBS with 1.25 mM Ca^{2+} for 1 minute, to enable comparable assessment of GTTR clearance. At the initial time point (Fig. 7A,D), GTTR levels in all KPT-pBabe and KPT2-TRPV4 cell lines were similar. After incubation in endolymph-like buffer for 5 or 10 minutes at 37°C to facilitate temperature-dependent TRPV4 activity, both cell lines had much lower GTTR levels that those at the initial time point (Fig. 7A-F). However, KPT2-TRPV4 cells showed significantly higher GTTR levels than those in KPT2-pBabe cells after 10 minutes (Fig. 7A-I), which was confirmed for all the three KPT2-pBabe and three KPT2-TRPV4 cell lines. The inward current induced by TRPV4 in the endolymph-like environment is likely to prevent cells from releasing GTTR. The GTTR clearance rate in KPT2-M680D

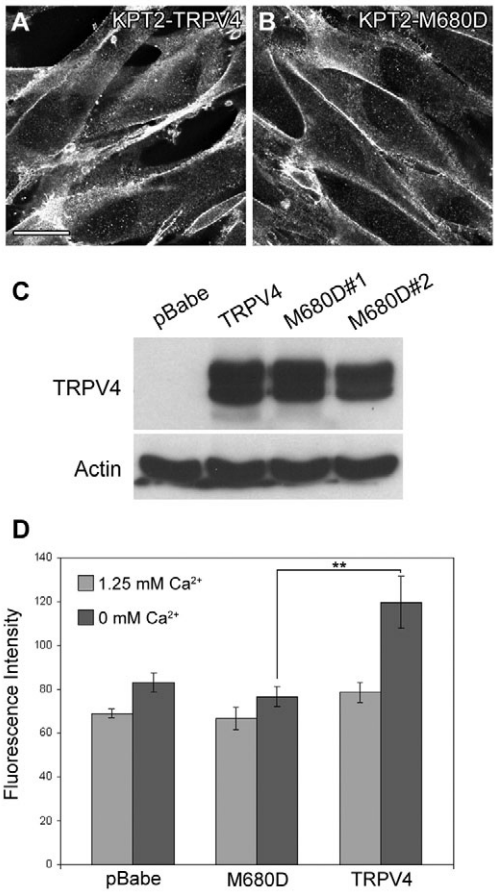

Fig. 6. GTTR uptake by TRPV4 is dependent on M680 residue within the channel pore. (A,B) KPT2-derived cell lines that express the M680D TRPV4 mutant were generated and tested for GTTR uptake. Immunofluorescence confirmed that the M680D TRPV4 mutant had normal membrane localization in the cells.(C,D) Immunoblotting showed similar protein expression levels of TRPV4 wild-type and the M680D mutant in KPT2-TRPV4 and the two KPT2-M680D clones (M680D#1 and #2), respectively. After 30 seconds of GTTR treatment, there was no significant enhancement in GTTR uptake by extracellular Ca^{2+} removal in KPT2-M680D cells, and similar results were obtained for the two KPT2-M680D cell lines (D). Fluorescence intensity data are shown as mean ± s.d. $^{**}P<0.01$. Scale bar, 20 μm.

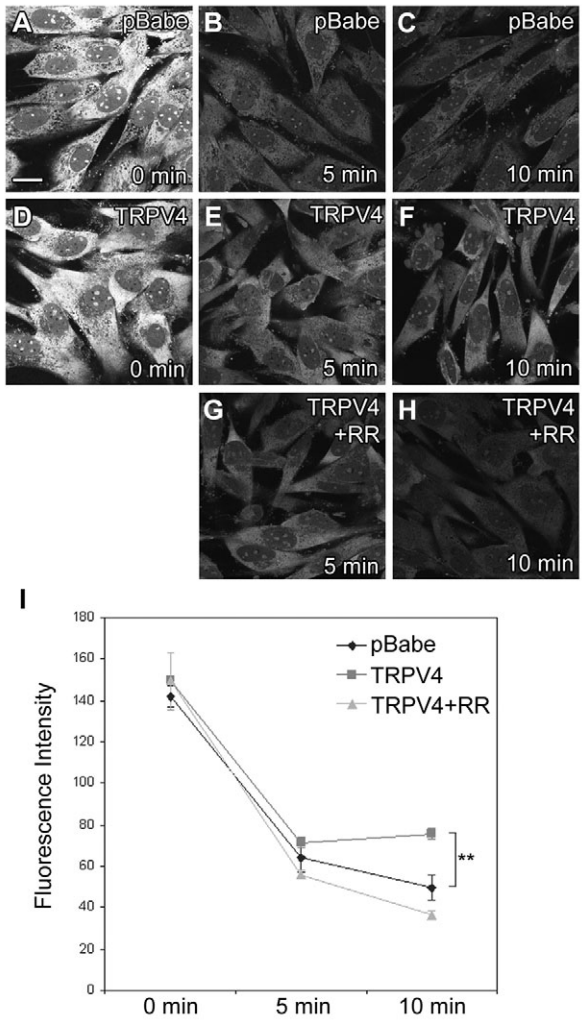

Fig. 7. TRPV4 contributes to GTTR retention in KPT2-TRPV4 cells in an endolymph-like extracellular environment. After 1 minute of GTTR treatment in PBS containing Ca^{2+} at 1.25 mM, KPT2-pBabe and KPT2-TRPV4 cells had similar levels of GTTR (A,D). After incubation in clearance buffer, KPT2-pBabe cells had lower GTTR fluorescence levels compared with KPT2-TRPV4 cells (B,C,E,F). Treatment with 10 μM RR to block inward currents accelerated GTTR clearance from KPT2-TRPV4 cells (G,H). Fluorescence intensity of cytoplasmic GTTR was quantified and statistically analyzed, and data are shown as mean ± s.d. (I). $^{**}P<0.01$. Scale bar, 20 μm.

cells was similar to KPT2-pBabe cells (data not shown), suggesting that GTTR retention in KPT2-TRPV4 cells depends on the permeability of the TRPV4 channel pore. In KPT2-TRPV4 cells, GTTR levels appeared slightly higher after 10 minutes than 5 minutes of clearance (Fig. 7E,F,I), possibly because cells started to contract to smaller sizes in response to the low-Ca^{2+} environment and GTTR became more concentrated in the cells. In extracellular buffer similar to DMEM (high Na^{+}, low K^{+}, high Ca^{2+}), no significant difference in GTTR clearance was seen between KPT2-pBabe and KPT2-TRPV4, confirming that the TRPV4-dependent GTTR retention requires an endolymph-like extracellular environment (data not shown). Since RR is known to block the inward current of cations induced by TRPV4, but not the outward current (Voets et al., 2002), cells were treated with RR during GTTR clearance to block the inward current. In the presence of 10 μM RR in endolymph-like buffer, GTTR clearance was significantly accelerated in KPT2-TRPV4 (Fig. 7G,H). These results suggest that, in an endolymph-like extracellular environment, aminoglycoside clearance is attenuated from cells that express TRPV4.

Discussion

Further insight into aminoglycoside uptake mechanisms is essential to better understand the selective cytotoxicity of these drugs in the inner ear and kidney, which remains a major clinical issue. Aminoglycoside uptake occurs by endocytosis in kidney and sensory hair cells (Sandoval et al., 2000; Hashino et al., 1997). However, aminoglycosides also enhance the generation of reactive oxygen species in euthermic cells at room temperature within seconds of drug exposure (Hirose et al., 1997) – too fast to be accounted for by endocytosis (Mamdouh et al., 1996). We have previously reported evidence that aminoglycoside uptake also occurs by non-endocytotic mechanisms and, more specifically, by cation-channel permeation (Myrdal et al., 2005; Myrdal and Steyger, 2005).

The GTTR conjugate has proven to be useful in studying the endocytosis of aminoglycosides and their subsequent intracellular trafficking (Sandoval et al., 2000; Sandoval and Molitoris, 2004).

Although the relative molecular mass of GTTR is larger than that of untagged gentamicin, this does not affect its ability to permeate directly into the cytoplasm, and its distribution has been verified by using gentamicin immunocytochemistry (Myrdal et al., 2005). By using GTTR, we have previously shown that aminoglycoside uptake in kidney cells can be regulated by membrane potential, pH, extracellular cations (Ca^{2+}, Gd^{3+}, La^{3+}), and non-specific cation channel blocker RR (Myrdal et al., 2005; Myrdal and Steyger, 2005). Importantly, TRPV1 activators resiniferatoxin and anandamide enhance aminoglycoside uptake in Madin-Darby canine kidney (MDCK) cells (Myrdal et al., 2005). However, TRPV1 expression is relatively low in the kidney and stria vascularis (Sanchez et al., 2001; Wang et al., 2004; Takumida et al., 2005), although there is substantial expression in hair cells (Zheng et al., 2003; Takumida et al., 2005). By contrast, TRPV4 is a TRP channel that is highly expressed in the kidney, stria vascularis, and hair cells (Liedtke et al., 2000; Strotmann et al., 2000; Wissenbach et al., 2000; Delany et al., 2001; Takumida et al., 2005; Shen et al., 2006). It has been suggested that TRPV4 responds to changes in interstitial osmolarity (e.g. changes in the urine-flow rate), and transmits the tonicity signals to more distal tubule segments where the finely tuned regulation of salt and water balance takes place (Cohen, 2005). In the inner ear, TRPV4 expression in the stria vascularis has been thought to have a role in maintaining the ionic composition of the endolymph and also the endocochlear potential (Liedtke et al., 2000). It has been hypothesized that aminoglycosides take a transstrial pathway to cross the stria vascularis and enter endolymph (Dai and Steyger, 2008). Therefore, we sought to determine whether TRPV4 is involved in cochlear trafficking of aminoglycosides.

Virtually all cells take up aminoglycosides, and most clear the drugs (Dai et al., 2006). However, the kidney and inner ear retain aminoglycosides and are susceptible to aminoglycoside-induced toxicity. They also share other common characteristics, such as fluid and ion regulation, and protein expression of various ion channels and transporters (Lang et al., 2007). Therefore, we used kidney cells as an in vitro model to study aminoglycoside uptake and clearance. Existing kidney proximal and distal tubule cell lines, such as opossum kidney (OK) and MDCK cells, are from different species, genetic backgrounds and were generated by different methods. For this reason, we developed new kidney proximal and distal tubule cell lines from mice that have similar genetic backgrounds by spontaneous immortalization. In support of our method of cell line generation, immortalized kidney proximal and distal tubule cell lines tend to retain differentiated-cell-specific functions (Vandewalle, 2002).

Cellular GTTR-uptake mechanisms

GTTR uptake was greater in KPT2 cells than in KDT3 cells in the presence of extracellular Ca^{2+}. Removal of extracellular Ca^{2+} increased GTTR uptake levels in KPT2 and KDT3 cells, with significantly greater enhancement in KDT3. Since removing extracellular Ca^{2+} increases inward currents mediated by TRPV4 (Voets et al., 2002), TRPV4 might be largely responsible for the enhanced GTTR uptake in KDT3 cells. In KDT3 cells, TRPV4 is highly expressed in the basolateral membrane, but there is also some expression in the apical membrane (Fig. 2G). This suggests that apical TRPV4 channels participates in GTTR uptake mechanisms in the absence of extracellular Ca^{2+}. In physiological extracellular Ca^{2+}, tight junctions near the lumenal surface of KDT3 cells might restrict GTTR access to TRPV4 in the basolateral membrane. It is possible that extracellular Ca^{2+} removal opened tight junctions (Pitelka et al., 1983), providing GTTR access to the basolateral membrane of KDT3 cells to allow greater GTTR uptake through TRPV4 channels.

KPT2 cells take up more GTTR than KDT3 cells in the presence of extracellular Ca^{2+}, and show modest enhancement of GTTR uptake when extracellular Ca^{2+} is removed. Since KPT2 cells lack TRPV4, they probably express other cation channels that are involved in GTTR uptake. TRPV1 and the purinergic $P2X_2$ receptor might be such channels because they are permeable to a large cationic dye FM1-43 (Meyers et al., 2003); however, we did not detect TRPV1 in KPT2 by immunoblot analysis (T.K. and P.S.S., unpublished data). These channels might also mediate a moderate increase in inward currents upon the removal of extracellular Ca^{2+}, and could therefore mediate GTTR uptake in KPT2 cells. Inhibition of GTTR uptake by RR in KPT2 cells also implicates other channels involved in GTTR uptake. Similar GTTR uptake levels in KPT2 and KDT3 cells in the absence of extracellular Ca^{2+} suggest that there are sufficient uptake routes at the cell membrane for GTTR and that virtually no barrier exists to block GTTR entry.

To determine whether TRPV4 has a role in aminoglycoside uptake in TRPV4-expressing cells, we generated KPT2-derived cell lines that express TRPV4 (KPT2-TRPV4) and control cell lines with empty vector (KPT2-pBabe), and compared GTTR uptake levels between these cell lines. Although KPT2-TRPV4 cells take up more GTTR when extracellular Ca^{2+} is removed, and although they can respond to the TRPV4 activator 4α-PDD in the Fura-2 ratiometry assay, we did not observe enhanced GTTR uptake when treating KPT2-TRPV4 cells with 4α-PDD (data not shown). In the presence of extracellular Ca^{2+}, 4α-PDD induces an inward current that is rapidly inactivated by intracellular Ca^{2+} (Nilius et al., 2004). It is possible that the duration of the inward current induced by 4α-PDD is not sufficient to enhance GTTR uptake in the presence of extracellular Ca^{2+}. It is also possible that the effect induced by 4α-PDD is too slow to appear during the GTTR treatment. In the absence of extracellular Ca^{2+}, the inward current induced by 4α-PDD lasts for several minutes (Nilius et al., 2004). However, removal of extracellular Ca^{2+} itself induces a large inward current (Voets et al., 2002), which is probably the reason why additive effects owing to 4α-PDD and extracellular Ca^{2+} removal were not observed for GTTR uptake.

In TRPV4, the methionine residue at position 680 (M680) is located within the K^+-channel-signature sequence – the crucial pore region of K^+ channels (Doyle et al., 1998; Zhou et al., 2001). The M680D point mutation abolishes Ca^{2+} selectivity of the TRPV4 pore (Voets et al., 2002). We found that removal of extracellular Ca^{2+} does not significantly enhance GTTR uptake in KPT2-derived cell lines that express the M680D TRPV4 mutant. This strongly indicates that, in KPT2-TRPV4 cells, GTTR permeates through the TRPV4 channel, because the mutation appears to only affect the channel-pore properties, and the mutant in KPT2-M680D cells is expressed at similar levels and localization compared with the wild-type channel in KPT2-TRPV4 cells.

Cochlear mechanisms of aminoglycoside uptake

In vivo, aminoglycosides are likely to enter hair cells from endolymph using both endocytosis and mechanoelectrical transduction channels (Hashino and Shero, 1995; Hiel et al., 1992; Marcotti et al., 2005). The mechanoelectrical transduction channel is permeable to dihydrostreptomycin and this permeation is attenuated by 1.3 mM extracellular Ca^{2+}, and enhanced at low levels of extracellular Ca^{2+} (Marcotti et al., 2005). Although it is yet to

be determined whether or not TRPV4 is a part of the mechanoelectrical channel, hair cells express TRPV4 in their apical membranes and stereocilia (Fig. 1) (Liedtke et al., 2000; Takumida et al., 2005; Shen et al., 2006). It is interesting to speculate that TRPV4 in the apical membrane of hair cells, including stereocilia, facilitates rapid aminoglycoside uptake into the cells due to the ultra-low Ca^{2+} environment in endolymph (Lang et al., 2007).

In this study, we also showed that aminoglycoside clearance is attenuated from cells that express TRPV4 in an endolymph-like extracellular environment. The large inward current induced by TRPV4 might prevent cell from releasing aminoglycosides. KPT2-M680D cells did not show TRPV4-dependent GTTR retention, supporting the idea that TRPV4 channel activity is responsible for aminoglycoside retention. It is possible that TRPV4 or other TRP channels expressed in the apical membrane contribute to aminoglycoside retention in hair cells. TRPV4 is not likely to have a role in aminoglycoside retention in most other cells, including kidney distal tubule cells, because there was no TRPV4-dependent GTTR retention in cells incubated in buffer that was similar to the typical extracellular ion components (such as Dulbecco's modified Eagle's medium, DMEM).

Although the stria vascularis of the inner ear is not thought to be as susceptible as hair cells, aminoglycosides can also damage the stria vascularis (Forge and Fradis, 1985; Kusunoki et al., 2004), which in turn leads to auditory dysfunction. In the stria vascularis, we identified high levels of TRPV4 protein in the lumenal membrane of marginal cells, bathed in endolymph (Fig. 1). Therefore, it is possible that TRPV4 channels contribute to aminoglycoside retention in the stria vascularis by preventing drug clearance from endolymph.

A better understanding of aminoglycoside permeation through TRPV4 and other non-selective cation channels will further our knowledge of how systemic aminoglycosides enter the cochlear fluids and hair cells. This will enable the development of new strategies to block aminoglycoside entry in these cells, and prevent aminoglycoside-induced hearing loss and vestibular disorders following systemic administration.

Materials and Methods

Cell culture

Mouse kidney cell lines were generated as described previously (Turker et al., 1999). Briefly, mouse kidney was minced using a surgical blade, digested with 0.07 mg/ml Liberase Blenzyme (Roche Diagnostics Corp.) at 37°C for 45 minutes and spun down. Cells were resuspended in DMEM supplemented with 15% FBS, and plated in 100-mm plates to obtain primary cultures. Primary cultures were maintained in DMEM with 15% FBS, and several clones were expanded to identify cells that had undergone spontaneous immortalization. Two kidney proximal and one distal tubule cell lines were identified based on morphology and TRPV4 expression, and designated as KPT1, KPT2 and KDT3, respectively. These cell lines were maintained in DMEM with 10% FBS. KPT2-derived cell lines generated by retroviral transduction were maintained in 2.5 μg/ml puromycin-containing DMEM with 10% FBS. Madin-Darby canine kidney cells (MDCK) were maintained in MEM alpha modification with 10% FBS.

Reverse transcriptase (RT)-PCR

Total RNA from cells was isolated by using RNeasy Mini kit (Qiagen), and first-strand cDNA was synthesized from 1 μg of total RNA in a 20 μl reaction mixture containing oligo(dT) to hybridize to 3′ poly(A) tails of mRNA, and SuperScript II reverse transcriptase (Invitrogen) to catalyze synthesis. The RNA template was removed after cDNA synthesis by digestion with RNase H. For PCR, 2 μl of the reverse-transcribed cDNA was used in each reaction catalyzed by AmpliTaq DNA polymerase (Applied Biosystems). The PCR condition used were 95°C for 2 minutes followed by 35 cycles of 95°C for 30 seconds, 60°C for 30 seconds, and 72°C for 1 minute for all reactions. Primers were 5′-CCTTCGTGCTCCTGTTGAAC-3′ and 5′-CACCACTTC-ATCTGCGCTTG-3′ for mouse TRPV4 (410 bp fragment), 5′-TGTTGC-TCTAGACTTCGAGCAG-3′ and 5′-ACCGATCCACACAGAGTACTTG-3′ for mouse β-actin (373 bp fragment). PCR was performed in an Applied Biosystems thermal cycler. PCR products were analyzed by electrophoresis in 2% agarose gel.

Immunoblotting

Total proteins were extracted with lysis buffer (50 mM Tris at pH 7.5, 150 mM NaCl, 5 mM EDTA, 1% Triton X-100, 0.5% sodium deoxycholate) that contained protease inhibitor cocktail (Sigma). Extracts were centrifuged at 14,000 ***g*** to remove cell debris, mixed with SDS sample buffer, and separated by 8% SDS-PAGE. The proteins were transferred to PVDF membranes (Millipore). The membrane was blocked with 5% non-fat dry milk in Tris-buffered saline containing 0.1% Tween 20 (TBST) for 1 hour and then incubated with TRPV4 antibody (a generous gift from Stefan Heller, Stanford University, Palo Alto, CA) at 1:5000 dilution, or actin antibody (Sigma) at 1:500 dilution overnight at 4°C. The blots were washed three times with TBST, incubated with horseradish peroxidase-conjugated secondary antibody for 1 hour at room temperature and washed again three times. The protein bands were detected by chemi-luminescence using SuperSignal West Dura Extended Duration Substrate (Pierce).

Immunofluorescence

To generate whole mounts and sections of the murine cochlea and kidney for immunolabeling, mice were fixed by transcardiac perfusion of 4% paraformaldehyde in PBS, excised and immersion fixed overnight with 4% paraformaldehyde plus 0.5% Triton X-100 (FATX). The cochlea was dissected and lateral wall exposed, and bone was removed from the stria vascularis. The kidney was vibratome-sectioned at 100 μm thickness. Tissues and sections were blocked with PBS containing 10% normal goat serum and 1% BSA, incubated with rabbit TRPV4 antibody at 1:2000 dilution for 1 hour, and then with Alexa-Fluor-488-conjugated goat anti-rabbit antibody for 1 hour, prior to washing, labeling with Alexa-Fluor-568 phalloidin at 1:100 for 1 hour. Specimens were then washed, fixed with 4% paraformaldehyde, rinsed and mounted using VectaShield, and imaged using confocal microscopy (Steyger et al., 2003).

Retroviral tranduction

Rat TRPV4 cDNA (a generous gift from Wolfgang Liedtke, Duke University, Durham, NC) in pcDNA3.1 was amplified by PCR, using *PfuUltra* DNA polymerase (Stratagene) and the primers 5′-TTTGGATCCACCATGGCAGATCCTGGTGATG-3′ and 5′-TTTGTCGACTACAGTGGTGCGTCCTCCGC-3′. The PCR product was digested with *Bam*HI and *Sal*I, and subcloned into a retroviral expression plasmid pBabe-puro. To introduce the M680D point mutation in TRPV4, QuikChange Site-Directed Mutagenesis Kit (Stratagene) with primers 5′-CAAGCTCACCATCG-GCGACGGCGACCTGGAGATGC-3′ and 5′-GCATCTCCAGGTCGCCGTCG-CCGATGGTGAGCTTG-3′ were used to generate the point mutation. The resultant plasmids were sequenced to confirm that there is no false mutation within the coding region of TRPV4. Each retroviral expression construct or the pBabe-puro control plasmid was transfected into Phoenix Eco packaging cells by using LipofectAMINE 2000 (Invitrogen). After 72 hours, the retrovirus-containing supernatant was collected, diluted (1:1000) with growth medium (DMEM with 10% FBS) and added to KPT2 cell cultures. This medium was removed after 24 hours, and growth medium supplemented with puromycin (2.5 μg/ml) was added to select for retrovirus-infected cells. From dozens of surviving cells after several days of puromycin treatment, several clones were selected and expanded.

Measurement of intracellular Ca^{2+} by using Fura-2 ratiometry

Cells were trypsinized, washed, and resuspended in 10 ml of HBSS (130 mM NaCl, 4.7 mM KCl, 1.25 mM $CaCl_2$, 1.18 mM $MgSO_4$, 5 mM glucose, 15 mM HEPES pH 7.5) supplemented with 2 μM Fura-2-AM and 100 μl of 2% Pluronic F-127 (20% stock solution in DMSO, Molecular Probes, Inc.) per 100 mm dish, and then incubated for 45 minutes at 37°C. Cells were pelleted at 1,000 ***g*** for 5 minutes at 25°C, resuspended with 1-2 ml of HBSS to achieve final concentration of ~$2\text{-}8\times10^7$ cells/ml, and maintained on ice for 30 minutes. The suspended Fura-2-loaded cells (50 μl) were assayed for intracellular Ca^{2+} concentration in a cuvette filled with pre-warmed (37°C) HBSS under constant gentle stirring (2 ml final volume) as previously reported (Xu et al., 2003). Fluorescent emission was monitored at 510 nm and recorded once per second in the presence of alternating excitation at 340 nm and 380 nm using a Hitachi F-2500 fluorescence spectrophotometer (Hitachi Instruments, Inc.). For treatment with the TRPV4 agonist 4α-phorbol 12,13-didecanoate (4α-PDD), the agonist was added directly to the cuvette in a small volume at final concentration of 50 nM, after a stable baseline fluorescence ratio had been achieved (not shown in figure). For treatment with hypotonicity, cells were added directly to hypotonic HBSS (150 mOsmol/kgH_2O). Calibration of the Fura-2 signal was performed as previously described (Roullet et al., 1997) using the Fura-2–Ca^{2+} dissociation constant of 224 nM (Grynkiewicz et al., 1985).

Gentamicin–Texas-Red uptake and clearance, and confocal microscopy

Gentamicin-Texas Red (GTTR) was generated as described previously (Myrdal et al., 2005). Cells plated on 8-well chambered coverslips were washed with PBS with or without 1.25 mM $CaCl_2$ twice, incubated with 5 μg/ml GTTR in PBS with or without 1.25 mM $CaCl_2$ for 30 seconds at room temperature to preclude endocytosis. Cells were washed again with PBS three times to remove GTTR from extracellular buffer, and fixed with FATX for 45 minutes. For Ruthenium Red (RR) treatment, RR was added to GTTR solution at the final concentration of 50 μM before cells were treated with GTTR. For GTTR clearance, cells were treated with GTTR for

1 minute under the same conditions as for GTTR uptake. After washing with PBS three times, cells were incubated in clearance buffer (1.3 mM NaCl, 130 mM KCl, 30 mM $KHCO_3$, 0.05 mM $CaCl_2$, pH 7.5) with or without 10 μM RR for 5 or 10 minutes at 37°C prior to fixation with FATX. Buffer similar to DMEM was also tested for GTTR clearance, with components of 110 mM NaCl, 5.3 mM KCl, 44 mM $NaHCO_3$, 1.8 mM $CaCl_2$, 0.9 mM NaH_2PO_4, adjusted to pH 7.5. The distribution of GTTR fluorescence was examined using an 8-bit Bio-Rad 1024 ES scanning laser system. For each individual set of images to be compared, the same confocal settings were used, and two images per well were collected. There were two wells per experimental condition, and each experiment was performed at least three times, to confirm that the results were consistent. GTTR fluorescent intensity values were obtained by histogram function of the ImageJ software after removal of nuclei and intercellular pixels using Adobe Photoshop. Fluorescence intensity was compared only within each set of images or experiment, and was not compared between different experiments because different image acquisition settings were used for different experiments to obtain the best dynamic range.

We thank Stefan Heller for anti-TRPV4 antibody and Wolfgang Liedtke for TRPV4 cDNA and TRPV4-knockout mice. This work was supported by NIH NIDCD grants DC04555 (P.S.S.), P30 DC05983, T32 DC005945 and F32 DC008465 (T.K.), and by the Oregon Medical Research Foundation.

References

Chen, P. and Segil, N. (1999). p27(Kip1) links cell proliferation to morphogenesis in the developing organ of Corti. *Development* **126**, 1581-1590.

Cohen, D. M. (2005). TRPV4 and the mammalian kidney. *Pflugers Arch.* **451**, 168-175.

Dai, C. F. and Steyger, P. S. (2008). A systemic gentamicin pathway across the stria vascularis. *Hear. Res.* **235**, 114-124.

Dai, C. F., Mangiardi, D., Cotanche, D. A. and Steyger, P. S. (2006). Uptake of fluorescent gentamicin by vertebrate sensory cells in vivo. *Hear. Res.* **213**, 64-78.

Davies, J. and Davis, B. D. (1968). Misreading of ribonucleic acid code words induced by aminoglycoside antibiotics. The effect of drug concentration. *J. Biol. Chem.* **243**, 3312-3316.

Delany, N. S., Hurle, M., Facer, P., Alnadaf, T., Plumpton, C., Kinghorn, I., See, C. G., Costigan, M., Anand, P., Woolf, C. J. et al. (2001). Identification and characterization of a novel human vanilloid receptor-like protein, VRL-2. *Physiol. Genomics* **4**, 165-174.

Doyle, D. A., Morais Cabral, J., Pfuetzner, R. A., Kuo, A., Gulbis, J. M., Cohen, S. L., Chait, B. T. and MacKinnon, R. (1998). The structure of the potassium channel: molecular basis of K+ conduction and selectivity. *Science* **280**, 69-77.

Forge, A. and Fradis, M. (1985). Structural abnormalities in the stria vascularis following chronic gentamicin treatment. *Hear. Res.* **20**, 233-244.

Forge, A. and Schacht, J. (2000). Aminoglycoside antibiotics. *Audiol. Neurootol.* **5**, 3-22.

Grohskopf, L. A., Huskins, W. C., Sinkowitz-Cochran, R. L., Levine, G. L., Goldmann, D. A. and Jarvis, W. R. (2005). Use of antimicrobial agents in United States neonatal and pediatric intensive care patients. *Pediatr. Infect. Dis. J.* **24**, 766-773.

Grynkiewicz, G., Poenie, M. and Tsien, R. Y. (1985). A new generation of Ca^{2+} indicators with greatly improved fluorescence properties. *J. Biol. Chem.* **260**, 3440-3450.

Hashino, E. and Shero, M. (1995). Endocytosis of aminoglycoside antibiotics in sensory hair cells. *Brain Res.* **704**, 135-140.

Hashino, E., Shero, M. and Salvi, R. J. (1997). Lysosomal targeting and accumulation of aminoglycoside antibiotics in sensory hair cells. *Brain Res.* **777**, 75-85.

Hiel, H., Schamel, A., Erre, J. P., Hayashida, T., Dulon, D. and Aran, J. M. (1992). Cellular and subcellular localization of tritiated gentamicin in the guinea pig cochlea following combined treatment with ethacrynic acid. *Hear. Res.* **57**, 157-165.

Hirose, K., Hockenbery, D. M. and Rubel, E. W. (1997). Reactive oxygen species in chick hair cells after gentamicin exposure in vitro. *Hear. Res.* **104**, 1-14.

Klein, J. O. (1984). Recent advances in management of bacterial meningitis in neonates. *Infection* **12 Suppl. 1**, S44-S51.

Kusunoki, T., Cureoglu, S., Schachern, P. A., Sampaio, A., Fukushima, H., Oktay, M. F. and Paparella, M. M. (2004). Effects of aminoglycoside administration on cochlear elements in human temporal bones. *Auris Nasus Larynx* **31**, 383-388.

Lang, F., Vallon, V., Knipper, M. and Wangemann, P. (2007). Functional significance of channels and transporters expressed in the inner ear and kidney. *Am. J. Physiol. Cell Physiol.* **293**, C1187-C1208.

Lee, J. E., Nakagawa, T., Kim, T. S., Iguchi, F., Endo, T., Kita, T., Murai, N., Naito, Y., Lee, S. H. and Ito, J. (2004). Signaling pathway for apoptosis of vestibular hair cells of mice due to aminoglycosides. *Acta Otolaryngol.* **Suppl. 551**, 69-74.

Liedtke, W., Choe, Y., Marti-Renom, M. A., Bell, A. M., Denis, C. S., Sali, A., Hudspeth, A. J., Friedman, J. M. and Heller, S. (2000). Vanilloid receptor-related osmotically activated channel (VR-OAC), a candidate vertebrate osmoreceptor. *Cell* **103**, 525-535.

Lowenheim, H., Furness, D. N., Kil, J., Zinn, C., Gultig, K., Fero, M. L., Frost, D., Gummer, A. W., Roberts, J. M., Rubel, E. W. et al. (1999). Gene disruption of p27(Kip1) allows cell proliferation in the postnatal and adult organ of corti. *Proc. Natl. Acad. Sci. USA* **96**, 4084-4088.

Mamdouh, Z., Giocondi, M. C., Laprade, R. and Le Grimellec, C. (1996). Temperature dependence of endocytosis in renal epithelial cells in culture. *Biochim. Biophys. Acta* **1282**, 171-173.

Marcotti, W., van Netten, S. M. and Kros, C. J. (2005). The aminoglycoside antibiotic dihydrostreptomycin rapidly enters mouse outer hair cells through the mechano-electrical transducer channels. *J. Physiol.* **567**, 505-521.

Meyers, J. R., MacDonald, R. B., Duggan, A., Lenzi, D., Standaert, D. G., Corwin, J. T. and Corey, D. P. (2003). Lighting up the senses: FM1-43 loading of sensory cells through nonselective ion channels. *J. Neurosci.* **23**, 4054-4065.

Mingeot-Leclercq, M. P. and Tulkens, P. M. (1999). Aminoglycosides: nephrotoxicity. *Antimicrob. Agents Chemother.* **43**, 1003-1012.

Myrdal, S. E. and Steyger, P. S. (2005). TRPV1 regulators mediate gentamicin penetration of cultured kidney cells. *Hear. Res.* **204**, 170-182.

Myrdal, S. E., Johnson, K. C. and Steyger, P. S. (2005). Cytoplasmic and intra-nuclear binding of gentamicin does not require endocytosis. *Hear. Res.* **204**, 156-169.

Nilius, B., Vriens, J., Prenen, J., Droogmans, G. and Voets, T. (2004). TRPV4 calcium entry channel: a paradigm for gating diversity. *Am. J. Physiol. Cell Physiol.* **286**, C195-C205.

Noller, H. F. (1991). Ribosomal RNA and translation. *Annu. Rev. Biochem.* **60**, 191-227.

Pirvola, U., Xing-Qun, L., Virkkala, J., Saarma, M., Murakata, C., Camoratto, A. M., Walton, K. M. and Ylikoski, J. (2000). Rescue of hearing, auditory hair cells, and neurons by CEP-1347/KT7515, an inhibitor of c-Jun N-terminal kinase activation. *J. Neurosci.* **20**, 43-50.

Pitelka, D. R., Taggart, B. N. and Hamamoto, S. T. (1983). Effects of extracellular calcium depletion on membrane topography and occluding junctions of mammary epithelial cells in culture. *J. Cell Biol.* **96**, 613-624.

Roullet, J. B., Luft, U. C., Xue, H., Chapman, J., Bychkov, R., Roullet, C. M., Luft, F. C., Haller, H. and McCarron, D. A. (1997). Farnesol inhibits L-type Ca^{2+} channels in vascular smooth muscle cells. *J. Biol. Chem.* **272**, 32240-32246.

Sanchez, J. F., Krause, J. E. and Cortright, D. N. (2001). The distribution and regulation of vanilloid receptor VR1 and VR1 5′ splice variant RNA expression in rat. *Neuroscience* **107**, 373-381.

Sandoval, R. M. and Molitoris, B. A. (2004). Gentamicin traffics retrograde through the secretory pathway and is released in the cytosol via the endoplasmic reticulum. *Am. J. Physiol. Renal Physiol.* **286**, F617-F624.

Sandoval, R. M., Dunn, K. W. and Molitoris, B. A. (2000). Gentamicin traffics rapidly and directly to the Golgi complex in LLC-PK(1) cells. *Am. J. Physiol. Renal Physiol.* **279**, F884-F890.

Shen, J., Harada, N., Kubo, N., Liu, B., Mizuno, A., Suzuki, M. and Yamashita, T. (2006). Functional expression of transient receptor potential vanilloid 4 in the mouse cochlea. *NeuroReport* **17**, 135-139.

Steyger, P. S., Peters, S. L., Rehling, J., Hordichok, A. and Dai, C. F. (2003). Uptake of gentamicin by bullfrog saccular hair cells in vitro. *J. Assoc. Res. Otolaryngol.* **4**, 565-578.

Strotmann, R., Harteneck, C., Nunnenmacher, K., Schultz, G. and Plant, T. D. (2000). OTRPC4, a nonselective cation channel that confers sensitivity to extracellular osmolarity. *Nat. Cell Biol.* **2**, 695-702.

Taber, H. W., Mueller, J. P., Miller, P. F. and Arrow, A. S. (1987). Bacterial uptake of aminoglycoside antibiotics. *Microbiol. Rev.* **51**, 439-457.

Takeuchi, S., Ando, M., Sato, T. and Kakigi, A. (2001). Three-dimensional and ultrastructural relationships between intermediate cells and capillaries in the gerbil stria vascularis. *Hear. Res.* **155**, 103-112.

Takumida, M., Kubo, N., Ohtani, M., Suzuka, Y. and Anniko, M. (2005). Transient receptor potential channels in the inner ear: presence of transient receptor potential channel subfamily 1 and 4 in the guinea pig inner ear. *Acta Otolaryngol.* **125**, 929-934.

Tian, W., Salanova, M., Xu, H., Lindsley, J. N., Oyama, T. T., Anderson, S., Bachmann, S. and Cohen, D. M. (2004). Renal expression of osmotically responsive cation channel TRPV4 is restricted to water-impermeant nephron segments. *Am. J. Physiol. Renal Physiol.* **287**, F17-F24.

Turker, M. S., Gage, B. M., Rose, J. A., Elroy, D., Ponomareva, O. N., Stambrook, P. J. and Tischfield, J. A. (1999). A novel signature mutation for oxidative damage resembles a mutational pattern found commonly in human cancers. *Cancer Res.* **59**, 1837-1839.

Vandewalle, A. (2002). Immortalized renal proximal and collecting duct cell lines derived from transgenic mice harboring L-type pyruvate kinase promoters as tools for pharmacological and toxicological studies. *Cell Biol. Toxicol.* **18**, 321-328.

Voets, T., Prenen, J., Vriens, J., Watanabe, H., Janssens, A., Wissenbach, U., Bodding, M., Droogmans, G. and Nilius, B. (2002). Molecular determinants of permeation through the cation channel TRPV4. *J. Biol. Chem.* **277**, 33704-33710.

Wang, C., Hu, H. Z., Colton, C. K., Wood, J. D. and Zhu, M. X. (2004). An alternative splicing product of the murine trpv1 gene dominant negatively modulates the activity of TRPV1 channels. *J. Biol. Chem.* **279**, 37423-37430.

Watanabe, H., Davis, J. B., Smart, D., Jerman, J. C., Smith, G. D., Hayes, P., Vriens, J., Cairns, W., Wissenbach, U., Prenen, J. et al. (2002). Activation of TRPV4 channels (hVRL-2/mTRP12) by phorbol derivatives. *J. Biol. Chem.* **277**, 13569-13577.

Wissenbach, U., Bodding, M., Freichel, M. and Flockerzi, V. (2000). Trp12, a novel Trp related protein from kidney. *FEBS Lett.* **485**, 127-134.

Xu, H., Zhao, H., Tian, W., Yoshida, K., Roullet, J. B. and Cohen, D. M. (2003). Regulation of a transient receptor potential (TRP) channel by tyrosine phosphorylation. SRC family kinase-dependent tyrosine phosphorylation of TRPV4 on TYR-253 mediates its response to hypotonic stress. *J. Biol. Chem.* **278**, 11520-11527.

Zheng, J., Dai, C., Steyger, P. S., Kim, Y., Vass, Z., Ren, T. and Nuttall, A. L. (2003). Vanilloid receptors in hearing: altered cochlear sensitivity by vanilloids and expression of TRPV1 in the organ of corti. *J. Neurophysiol.* **90**, 444-455.

Zhou, Y., Morais-Cabral, J. H., Kaufman, A. and MacKinnon, R. (2001). Chemistry of ion coordination and hydration revealed by a K^+ channel-Fab complex at 2.0 Å resolution. *Nature* **414**, 43-48.